AD-A190 072 THE TIME-TEMPERATURE-TRANSFORMATION (TTT) DIAGRAM AS A BASIS FOR RELATING..(U) PRINCETON UNIV NJ DEPT OF CHEMICAL ENGINEERING J K GILLHAM JAN 88 TR-13 1/1

UNCLASSIFIED N00014-84-K-0021 F/G 7/6 NL

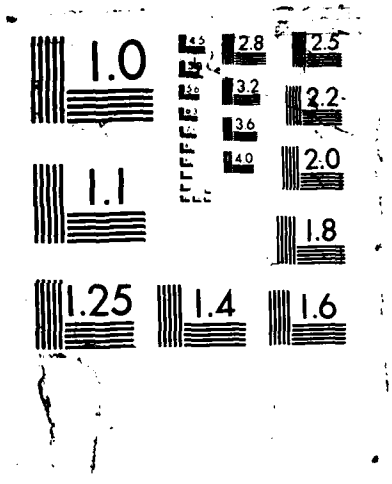
1.0
1.1
1.25
1.4
1.6
1.8
2.0
2.2
2.5
2.8
3.2
3.6
4.0

AD-A190 872

OFFICE OF NAVAL RESEARCH

Contract N00014-84-K-0021

Technical Report No. 13

The Time-Temperature-Transformation [TTT] Diagram as a Basis for Relating The Formation and Properties of Reactive Coatings

by

John K. Gillham

Presented as the Plenary Lecture
at the
Water-Borne and Higher Solids Coatings Symposium
February 3, 1988
New Orleans, LA, USA

Polymer Materials Program
Department of Chemical Engineering
Princeton University
Princeton, NJ 08544

January 1988

Reproduction in whole or in part is permitted for
any purpose of the United States Government

This document has been approved for public release
and sale; its distribution is unlimited

Principal Investigator
John K. Gillham
(609) 452-4694

DTIC
ELECTE
FEB 03 1988
S D
H

88 1 26 055

SECURITY CLASSIFICATION OF THIS PAGE (When Data Entered)

REPORT DOCUMENTATION PAGE

READ INSTRUCTIONS BEFORE COMPLETING FORM

1 REPORT NUMBER: Technical Report #13	2 GOVT ACCESSION NO: N/A
3 RECIPIENT'S CATALOG NUMBER: N/A	
4 TITLE (and Subtitle): The Time-Temperature-Transformation [TTT] Diagram as a Basis for Relating the Formation and Properties of Reactive Coatings	5 TYPE OF REPORT & PERIOD COVERED: 1/31/87 - 1/31/88
	6 PERFORMING ORG. REPORT NUMBER:
7 AUTHOR(s): J. K. Gillham	8 CONTRACT OR GRANT NUMBER(s): N00014-84-K-0021
9 PERFORMING ORGANIZATION NAME AND ADDRESS: Polymer Materials Program, Department of Chemical Engineering, Princeton University, Princeton, NJ 08544	10 PROGRAM ELEMENT, PROJECT, TASK AREA & WORK UNIT NUMBERS
11 CONTROLLING OFFICE NAME AND ADDRESS: Office of Naval Research, Attn: Code 413, 800 N. Quincy St., Arlington, VA 22217	12 REPORT DATE: January 1988
	13 NUMBER OF PAGES: 22
14 MONITORING AGENCY NAME & ADDRESS (if different from Controlling Office)	15 SECURITY CLASS. (of this report): Unclassified
	15a DECLASSIFICATION/DOWNGRADING SCHEDULE

16 DISTRIBUTION STATEMENT (of this Report):

Approved for public release; distribution unlimited.

Accession For	
NTIS GRA&I	☑
DTIC TAB	☐
Unannounced	☐
Justification	
By	
Distribution/	
Availability Codes	
Dist	Avail and/or Special
A-1	

17 DISTRIBUTION STATEMENT (of the abstract entered in Block 20, if different from Report):

N/A

18 SUPPLEMENTARY NOTES

QUALITY INSPECTED 2

19 KEY WORDS (Continue on reverse side if necessary and identify by block number):

Cure, Thermal Degradation, Density,
Vitrification, Kinetics,
Glass Transition, Time-Temperature-Transformation Cure Diagrams,
Solvent Evaporation, Torsional Braid Analysis

20 ABSTRACT (Continue on reverse side if necessary and identify by block number):

A review of research in the author's laboratory is presented. Interrelationships between reaction conditions and material properties of thermosetting and high T_g polymers are discussed from the point of view of a generalized time-temperature-transformation (TTT) diagram. The TBA torsion pendulum is discussed as a technique for characterizing reactive coatings.

DD FORM 1 JAN 73 1473 EDITION OF 1 NOV 65 IS OBSOLETE
S/N 0102-014-6601

SECURITY CLASSIFICATION OF THIS PAGE (When Data Entered)

THE TIME-TEMPERATURE-TRANSFORMATION [TTT] DIAGRAM AS A BASIS FOR RELATING THE FORMATION AND PROPERTIES OF REACTIVE COATINGS

John K. Gillham, Professor

Polymer Materials Program
Department of Chemical Engineering
Princeton University
Princeton, New Jersey 08544, USA

Presented at the
Water-Borne & Higher-Solids Coatings Symposium
February 3-5, 1988
New Orleans, LA, USA

Symposium Sponsored by
University of Southern Mississippi
Department of Polymer Science
and
Southern Society for Coatings Technology

ABSTRACT

A review of research in the author's laboratory is presented. Interrelationships between reaction conditions and material properties of thermosetting and high T_g polymers are discussed from the point of view of a generalized time-temperature-transformation (TTT) diagram. The TBA torsion pendulum is discussed as a technique for characterizing reactive coatings.

INTRODUCTION

This review of reserch in the author's laboratory, which is set into a general context, pertains principally to the formation and properties of high T_g polymeric glasses which are made by the transformation of liquid to amorphous solid by chemical reaction. The area is of particular importance in the making of composites, coatings, and adhesives by thermo-setting "cure" reactions in which multifunctional molecules of low molecular weight are converted into network macromolecules. An attempt has been made to produce a generalized model for the formation and properties of thermosetting systems which also incorporates linear systems: an example of the former is the cure of a neat epoxy resin; an example of the latter is the polymerization of neat styrene monomer below the glass transition of polystyrene. The review will therefore emphasize thermosetting systems with some reference to linear systems. The simplest model for chemical setting assumes a single reaction mechanism and no phase separation.

THE TIME-TEMPERATURE-TRANSFORMATION (TTT) ISOTHERMAL CURE DIAGRAM

A time-temperature-transformation (TTT) isothermal cure diagram (Fig. 1) may be used to provide an intellectual framework for understanding and comparing the cure and physical properties of thermosetting systems (1,2). The main features of such a diagram can be obtained by measuring the times to events that occur during isothermal cure at different temperatures, T_{cure}. These events include the onset of phase separation, gelation, vitrification, full cure, and devitrification. Phase separation may occur, for example, by precipitation of rubber from solution in rubber-modified formulations, or by the formation of monomer-insoluble oligomeric species and by the formation of gel particles (and also by crystallization in crystallizable systems). Molecular gelation corresponds to the incipient formation of an infinite molecular network, which gives rise to long range elastic behavior in the macroscopic fluid. It occurs at a definite conversion for a given system according to Flory's theory of gelation (3). After molecular gelation the material consists of normally miscible sol (finite molecular weight) and gel (infinite molecular weight) fractions, the ratio of the former to the latter decreasing with conversion. Vitrification occurs when the glass-transition temperature, T_g, rises to the temperature of cure. The material is liquid or rubbery when $T_{cure} > T_g$; it is glassy when $T_{cure} < T_g$. Devitrification occurs when the glass-transition temperature decreases through the cure temperature, as in thermal degradation. The diagram displays the distinct states encountered on cure due to chemical reactions. These states include liquid, sol/gel rubber, gel rubber (elastomer), ungelled (sol) glass, gelled glass, and char. The gelled glass region in the TTT cure diagram is divided into two parts by the full-cure line; in the absence of degradation (Fig. 1, devitrification and char), the top and lower parts can be designated fully cured gel glass and undercured sol/gel glass regions, respectively. The technological terms, A-, B- and C-stage resins correspond to sol glass, sol/gel glass, and fully cured gel

glass, respectively. The illustration also displays the critical temperatures $T_{g\infty}$, $_{gel}T_g$, and T_{go}, which are the glass-transition temperature of the fully cured system, the temperature at which molecular gelation and vitrification occur simultaneously, and the glass-transition temperature of the reactants, respectively.

Much of the behavior of thermosetting materials can be understood in terms of the TTT cure diagram through the influence of gelation, vitrification, and devitrification upon properties. Gelation retards macroscopic flow, and growth of a dispersed phase (eg, as in rubber-modified systems). Vitrification retards chemical conversion. Devitrification, due to thermal degradation, marks the lifetime for the material to support a substantial load.

The isothermal TTT cure diagram is more limited for the curing of linear rubber systems than for thermosetting systems because in practice only the region above $T_{g\infty}$ is relevant for the former. Gelation in the vulcanization of rubbers occurs at low conversions in comparison with typical thermo-setting systems.

The ungelled glassy state is the basis of commercial molding materials since, upon heating, the ungelled (sol) material flows before gelling through further reaction. Formulations can be processed as solids (eg, molding compositions) when T_{go} > ambient temperature; they can be processed as liquids (eg, as casting fluids) when T_{go} < ambient temperature.

The glass transition temperature of the material at the composition corresponding to molecular gelation is $_{gel}T_g$, since molecular gelation occurs as the material vitrifies when the temperature of cure is $_{gel}T_g$ (4). The molecular gelation curve (Fig. 1) therefore corresponds to $T_g = {}_{gel}T_g$. Temperature $_{gel}T_g$ is critical in determining the upper temperature for storing reactive materials to avoid gelation (which relates to "pot life"). However, cure below $_{gel}T_g$ eventually leads to gelation.

The morphology developed in two-phase systems, for example, those in which rubber-rich domains nucleate and grow as a dispersed phase in a curing rubber-modified thermoset, depends on the temperature of cure. The reaction temperature determines the competition between thermodynamic and kinetic (ie, transport) factors which affects the amount, the composition, and the distribution of dimensions of the dispersed phase. As an example, reaction at intermediate temperatures can result in a maximum in the amount of precipitated phase which may accompany a minimum in the time to the onset of phase separation (as shown in Fig. 1). For optimum mechanical properties, a two-phase system is cured first at one temperature to provide a particular morphology, and subsequently at a higher temperature to complete the reactions of the matrix (5,6). The $T_{g\infty}$ of the matrix will be determined by the extent of phase separation. A matrix parameter, the critical interparticle distance, has been reported (7) which determines the brittle to duc-

tile transition in rubber-modified thermoplastics. For a given volume fraction of a dispersed low-modulus phase the critical interparticle distance is determined by the particle size. This concept should be applicable to rubber-modified thermosets where cure under different conditions affects both the amount of phase separation and the particle size distribution.

In composite systems, shrinkage stresses due to volume contraction of the resin on isothermal cure begin to develop with adhesion of the curing resin to a rigid inclusion or substrate. This occurs after gelation above $_{gel}T_g$ and before vitrification below $_{gel}T_g$. The tensile stresses in the resin and the corresponding compressive stresses on an inclusion and substrate affect composite behavior. One consequence is fiber-buckling in resin/fiber composites. A related consequence of the shrinkage due to cure and the different coefficients of expansion and contraction of the constituents in brittle resin/fiber composites is the formation of spiral and helical cracks in the resin around isolated filaments and yarns (8,9). Their large surface areas per unit volume of matrix may contribute to the toughening of fiber/resin composites.

Prolonged isothermal cure at temperature T_{cure} below $T_{g\infty}$ would lead to $T_g = T_{cure}$ if the reactions were quenched by the process of vitrification. In practice, T_g is higher than T_{cure} because it can increase during the heating scan employed for measurement. Although vitrification has been defined to occur when $T_g = T_{cure}$, T_g, as usually measured, does not correspond to the glassy state, but rather to a state approximately halfway between the rubbery and glassy states; therefore reactions at T_{cure} continue beyond the assigned time to vitrification, which also results in $T_g > T_{cure}$. Furthermore, the extents to which reactions proceed in the glassy state depend on the influence of the glassy state on the reaction mechanism. However, even the intramolecular reactions involved in the imidization of polyamic acids to polyimides are restricted by the vitrification process, leading again to T_g being controlled by the temperature and the time of cure (11). In practice, for epoxies and polyimides, T_g is greater than T_{cure} by about 30-50°C after "normal" isothermal cure below $T_{g\infty}$ (10,11,12,13). This corresponds approximately to the half-width of the glass transition temperature region since T_g (as measured) increases through the isothermal temperature T_{cure} to about T_{cure} + 30 to 50°C after which the reaction rate is controlled by the low physical relaxation rates of the glassy state. The half-width of the glass transition region which is indicated in Figure 1 varies since the width of the glass transition depends on the value of T_g.

Correlations between macroscopic behavior and molecular structure of the reactants are most clearly defined in fully cured materials. Full cure is attained most readily by reaction above $T_{g\infty}$, and more slowly by curing below $T_{g\infty}$ to the full-cure line of the TTT cure diagram (12). The full cure line corresponds to $T_g = T_{g\infty}$.

In practice full cure is in general not a unique state because the state depends upon the time-temperature reaction path. In commonly used systems this is a consequence of competing chemical reactions with different activation energies. Furthermore, the time-temperature path of cooling after cure affects, for example, density and behavior at room temperature.

At high temperatures, non-curing chemical reactions result in degradation. Thermal degradation can result in devitrification as the glass-transition temperature decreases through the isothermal temperature due to a reduction in cross-linking or formation of plasticizing material. Degradation can also result in vitrification, eg, char formation (Fig. 1), as the glass-transition temperature increases through the isothermal temperature because of an increase in cross-linking or volatilization of low molecular weight plasticizing materials (13). In high T_g systems, cure and thermal degradation reactions compete. There is a need to obtain high temperature polymers from low temperature processing.

The limiting viscosity in the fluid state is controlled by molecular gelation above $_{gel}T_g$, and by vitrification below $_{gel}T_g$. At gelation, the weight-average molecular weight and zero shear-rate viscosity become infinite, although the number-average molecular weight is very low. Viscosity prior to vitrification below $_{gel}T_g$ is described by the Williams-Landel-Ferry (WLF) equation (14).

The time to reach a specified viscosity (Fig. 1) is often used as a practical method for measuring gelation times. Although this macroscopic isoviscosity approach is inconsistent with the molecular isoconversion theory of gelation, above temperature $_{gel}T_g$ the apparent activation energies obtained from the temperature dependence of the time to reach a specified viscosity approach the true activation energy for the chemical reactions leading to molecular gelation with increase of the specified viscosity (1).

The time to molecular gelation can be computed from the reaction kinetics and the conversion at molecular gelation, which is constant according to Flory's theory of gelation. The time to vitrification can be computed from the reaction kinetics and the conversion at vitrification (15,16,17), which increases with T_{cure}. Since vitrification occurs when the glass-transition temperature reaches the temperature of cure, computation of the time to vitrify requires knowledge of the relationship between T_g and conversion. Figure 2 shows that T_g increases with conversion at an increasing rate. In the absence of diffusion control, the simplest kinetic equation describing the reaction is

$$dX/dt = [A\exp(-E_A/RT)]f(X)$$

where X is the extent of reaction, E_A the activation energy, and the other characters have their usual significance. The times to molecular gelation and to vitrification can be computed versus tem-

perature using this equation when X_{gel} (for gelation), a relationship between X and T_g (for vitrification) (Fig. 2), and the reaction kinetics are known. The influence of diffusion control on the reaction rate can be deduced in principle from the differences between the experimentally measured and the computed gelation and vitrification curves.

The S-shaped vitrification curve obtained experimentally in the absence of thermal degradation has been matched by computation for one epoxy system from temperature T_{go} to temperature $T_{g\infty}$ (16).

The vitrification curve is generally S-shaped (17). At temperatures immediately above T_{go}, the time to vitrification passes through a maximum because of the opposing influences of the temperature dependences of the viscosity and the reaction rate constant. Immediately below $T_{g\infty}$, the time to vitrification passes through a minimum (18) because of the opposing influences of the temperature dependence of the reaction rate constant and the decreasing concentration of reactive sites at vitrification as $T_{g\infty}$ is approached. Knowledge of the minimum time and the corresponding temperature is useful in molding technology.

Cure of finite specimens at temperatures below that for the minimum time for vitrification (Fig. 1) can lead to the hotter inside vitrifying before the outside when the reaction is exothermic. Conversely, cure at higher temperatures can lead to the outside vitrifying before the inside: in this case internal stresses develop as the inside contracts relative to the vitrified outside due to the volume contraction of polymerization. The situation can be similar to the latter case when external heating causes the hotter outside to vitrify before the cooler inside. Similarly, cooling cured material from above $T_{g\infty}$ will lead to the outside vitrifying before the inside; internal stresses in this case will be minimized by cooling very slowly (i.e., annealing). These stresses, which are due to non-isothermal conditions in neat systems, are supplemented in composites by the differential shrinkage stresses which were referred to earlier in the article.

The conversion at vitrification can be computed in principle by relating the glass-transition temperature to contributions from the molecular weight and the cross-linking density, both of which vary with conversion (17). For polymerization prior to gelation (and for linear polymerization), the computation is simplified by the absence of cross-linking.

The fractional extent of reaction at vitrification and the time to vitrify, like molecular gelation, decrease with increasing functionality of the reactants (13). The effect of increasing functionality on molecular gelation, vitrification, and the temperatures $_{gel}T_g$, T_{go}, and $T_{g\infty}$ can be understood by considering the X-vs-T_g and the X_{gel} relationships, such as those in Figure 2. For example, the figure shows how temperature $_{gel}T_g$ for the material of lower functionality can be higher than that of higher functionality.

Increasing reaction time at any temperature leads to increasing conversion, T_g, average molecular weight, and cross-linking density. The modulus and density at the curing temperature also increase. However, upon cooling intermittently from the curing temperature to a temperature well below T_g, eg, room temperature (RT) for high T_g materials, the modulus (e.g., see Fig. 10) and density can decrease, whereas equilibrium absorption of water can increase with increasing extent of cure. This anomaly can result, for example, in a net expansion at room temperature when a reactive material which has been set at RT is post-cured at elevated temperatures and cooled to RT. A common basis for these interrelated phenomena is the increasing free volume at room temperature with increasing extent of cure (19).

The room temperature density (ρ_{RT}) actually passes through a maximum value with increasing conversion. Figure 3, which was constructed from series of isothermal cures followed by cooling slowly to RT, includes a master curve of ρ_{RT} versus T_g - RT (20). (In the absence of vitrification, T_g is a direct measure of conversion.) Perturbations from the master curve are due to isothermal vitrification which prevents the density from decreasing to the level of the master curve with increasing conversion. (It is difficult experimentally to obtain the complete master curve from one cure temperature since the reaction rate is too high at high temperatures of cure, and vitrification limits the extent of reaction below temperature $T_{g\alpha}$.) Vitrification nullifies the unique relationship between ρ_{RT} and T_g. The same value of T_g can then arise from different combinations of conversion and extent of physical annealing (aging); for example, a particular value of T_g can be obtained at lower temperatures with less conversion but more physical annealing. The limiting ρ_{RT} which corresponds to the highest T_g attained after long times at each temperature of cure depends on T_{cure} and varies inversely with T_{cure} (when $T_{cure} < T_{g\infty}$). When T_g is high the limiting ρ_{RT} will be stable at room temperature (if the cooling rate is slow). Although ρ_{RT} differences which can be obtained by curing to different extents is only about 0.5 percent, this corresponds to differences of about 20 percent in the free volume of the glass. It is not surprising therefore to observe corresponding changes of 20 percent in modulus and water absorption at room temperature. These concepts are relevant to the design of plastics with the dimensional stability needed for the replacement of metals by plastics.

One factor contributing to the maximum in ρ_{RT} versus conversion is summarized as follows (20). The value of ρ_{RT} depends on the contraction due to chemical reaction and the subsequent contraction due to cooling from T_{cure}. The latter involves contraction in the rubbery state (from T_{cure} to T_g) and contraction in the glassy state (from T_g to RT). With higher values of T_g there is less contraction on cooling since the coefficient of contraction of the rubbery state is higher than that of the glassy state. Since T_g rises nonlinearly with increasing conversion (Fig. 2), higher conversions

can give rise to less contraction on cooling from T_{cure}. The net sum of cure shrinkage and temperature shrinkage can therefore change from positive to negative with increasing conversion. The maximum in ρ_{RT} is associated with gelation and therefore with the glass transition temperature $_{gel}T_g$ at the composition corresponding to gelation since the non-linearity in T_g versus conversion relationship is amplified by the increase of crosslink density which occurs progressively after gelation with increasing conversion.

Another factor contributing to the ρ_{RT} decreasing with increasing conversion is the increasing relaxation times: during the transformation of liquid or rubber to glass this results in glasses which are progressively further from equilibrium. The higher T_g, the further from equilibrium a glass is at RT.

The concept of the TTT cure diagram can be extended to non-isothermal conditions for forming and annealing polymeric materials. For example, a continuous heating time-temperature-transformation (CHT) diagram results from heating a reactive system from (say) 25° to 300°C at a series of different rates of increasing temperature. The vitrification curve (i.e., $T_g = T$) will be joined to a devitrification curve (i.e., $T_g = T$) to form an envelope (21). This devitrification is a consequence of the rising glass transition temperature eventually not increasing at the same rate as the rate of rise of temperature. Such a diagram is useful in molding technology for defining time-temperature cure paths in which vitrification does not occur, for example, so as to obtain full cure. Conversely vitrification can be an essential part of a cure cycle so as to control reaction rates which could run out of control because of the exothermic nature of a reaction. The polymerization of 250 gallons of epoxy to encapsulate a magnetic coil in Princeton University's experimental Tokomak nuclear fusion reaction is accomplished by heating at a very low rate of temperature increase; the reaction rate is controlled in the process by the T_g increasing in concert with the temperature until $T_{g\infty}$, i.e., full cure, is attained.

LINEAR POLYMERIZATION AND THE TTT DIAGRAM

This section attempts, in a general manner, to incorporate linear polymerization of neat systems into the concept of the TTT diagram.

Difunctional liquid monomers can be transformed into glassy linear polymeric materials by reaction below the maximum glass transition temperature of the polymer, $T_{g\infty}$. The time to vitrification curve for the isothermal free radical polymerization of neat styrene versus the isothermal temperature of reaction, T_{rx}, has been computed in the absence of diffusion control (22). The calculation involved using the well established chemical kinetics from zero conversion to the conversion corresponding to $T_g = T_{rx}$. Since the neat mixture at any time consists of monomer and polymer (neglecting initiator and active chain radicals), the proportion of polymer to

monomer (i.e., the conversion) was calculated from the glass transition temperatures of the monomer (-100°C) and polymer (+100°C) and $T_g = T_{cure}$. The computed vitrification curves for the free-radical polymerization of styrene and for a linear-forming step-growth polymerization were S-shaped.

Phase separation can occur in neat linear polymerization as a consequence of insolubility of oligomer or polymer. This has been a particularly important consideration in the synthesis by step-growth polymerization of high T_g linear polymers, which of necessity have relatively inflexible chain structures. Precipitation often effectively removes the growing species from the reaction medium, thereby limiting the molecular weight. In the same type of polymerization the reaction temperature must be such that vitrification also does not occur (i.e. $T_{rx} > T_{g\infty}$). Phase separation can be analogous to vitrification in limiting molecular weight and T_g. (Use of exotic solvents overcomes the problems of insolubility and vitrification in the synthesis of high T_g rigid molecules: however, these solvents must be subsequently removed, often by ingeneous methods.)

Although chemical gelation does not occur in linear polymerization, long range elasticity can develop in the polymerizing fluid as the consequence of entanglements between polymer molecules. These will occur at lower conversions for chain reactions where high molecular weight polymer forms throughout the reaction, than for step-growth polymerizations where high molecular weight polymer develops only late in polymerization.

The situation is more complex for the conversion of liquid monomers into polymers which can crystallize. Polymerization of neat monomer above $T_{g\infty}$ can lead to solidification because of crystallization. (The maximum melting temperature, $T_{m\infty}$, is greater than the maximum glass transition temperature, $T_{g\infty}$.) Polymerization below $T_{g\infty}$ can lead to solidification as the result of vitrification or crystallization. The melting temperature range, as well as the glass transition temperature should be directly related to the temperature of reaction: it is well known that T_m of a linear polymer is directly related to the isothermal temperature of crystallization.

SOLVENT-BASED REACTIVE COATINGS AND THE TTT DIAGRAM

An important application of the transformation of reactive liquids to solids involves loss of solvent. In these vitrification can occur as the consequence of both solvent loss and chemical reaction (11). The following example demonstrates how the methodology of the TTT cure diagram has been used to characterize a particular solvent-based reactive coating (23). The summary isothermal TTT diagram is shown as Figure 4.

The particular system is reactive at reasonable rates only above $T_{g\infty}$ ($T_{g\infty} \simeq 147$°C). Cure involves volatilization of both

temperature is a) a direct measure of the state of cure (e.g., conversion), is b) used to define the vitrification contour, and c) is in itself the characteristic softening temperature of amorphous materials.

TP/TBA - MODES

The freely oscillating torsion pendulum can be used in two ways to characterize polymeric systems; these are the conventional torsion pendulum (TP) mode and the torsional braid analysis (TBA) mode, respectively (1). Geometrically simple specimens (e.g., films & filaments) are used in the TP mode to obtain quantitative values of the elastic and loss moduli. Impregnated braid specimens are used in the TBA mode to obtain transitions of polymers, to obtain a preliminary mechanical assessment of new polymers, and to characterize liquid to solid transformations (e.g. cure).

INSTRUMENTATION

A schematic diagram of the automated TBA torsion pendulum system which has been developed by the author is shown in Figure 5. The system is available from Plastics Analysis Instruments, Inc., Princeton, NJ 08540. The essence of the instrument is the inner pendulum assembly which is shown in Figure 6 and consists of a vertical specimen held in place with clamps attached to two rods. The upper activation rod is held vertically in alignment with a 2" Teflon sleeve and is rigidly attached to a horizontal gear which intermittently initiates free oscillations by computer-controlled stretching and releasing of a spring. The lower pendulum rod hangs freely and is magnetically coupled to a polaroid disc at its lower end.

The pendulum is enclosed in an air-tight cylindrical chamber (0.5" diameter), the atmosphere of which is closely controlled and monitored: inert, water-doped, and reactive gases have been used. There are no electronic devices within the specimen chamber. Dry helium, rather than nitrogen, is usually used as an inert atmosphere because of its higher thermal conductivity at cryogenic temperatures. An on-line electronic hygrometer is used to continuously monitor the water vapor content of atmospheres from < 20 to 20,000 ppm H_2O. A cylindrical copper block, wound around with cooling coils for liquid nitrogen and with band heaters, surrounds the specimen. Excellent temperature control is achieved by virtue of the large thermal mass of the copper block, with a temperature spread of <1°C over a 2" specimen. A temperature programmer/controller system permits experiments to be performed in isothermal (±0.1°C above 30°C) and dynamic modes from -190 to 400°C; in the dynamic mode the temperature may be increased or decreased linearly at controlled rates of 0.05 to 5°C/min. Cooling is achieved by controlling the flow of liquid nitrogen from a pressurized container. Routine temperature scans are made at rates of change of temperature of ±

2°C/minute. Measurements have been made as low as 4°K and as high as 700°C in modified apparatus.

A key factor in the instrumentation is the non-drag optical transducer which produces an electrical response that varies linearly with angular displacement. A polarizing disc is used as part of the inertial member of the pendulum, and a stationary second polarizer is positioned in front of a linearly-responding photocell. An analog electrical signal is obtained from a light beam passing through the pair of polarizers (Fig. 5).

The clamps on the pendulum allow a variety of specimens to be used: film, fiber, or coating on glass braid or foil substrate. Depending on the specimen, the system can be used as a conventional torsion pendulum or in the supported TBA mode. The substrate generally used in a TBA experiment is a loose, heat-cleaned glass braid containing about 3600 filaments. The specimen is prepared by simply dipping the braid into the neat liquid or into a solution of the material of interest dissolved in a solvent.

Quantitative values of the shear and loss moduli of polymer films are obtained from the natural frequency (~ 1 Hz) and damping of the induced oscillations of the torsion pendulum. Some advantages of using the torsion pendulum for the dynamic mechanical thermal analysis of polymers are its fundamental simplicity, its cost (less than $50,000), its utilization of the pendulum's resonance frequency (which means that the measurement is always made at the maximum sensitivity, since the specimen is a primary component of the pendulum), its use of a non-drag optical transducer (a pair of polarizers) which permits the use of small specimens (< 20 mg), and its free movement (because the pendulum is fixed only at one end, no adjustments for thermal expansion or contraction are required). In the torsional braid analysis (TBA) mode a glass braid (or other substrate) is impregnated with a polymer solution or polymer "melt", and measurements are made on the composite specimen. Although the specimen's relative rigidity is obtained instead of its shear modulus, the transition temperatures can readily be identified. The advantages of the TBA technique include ease of specimen fabrication, vertical self-alignment (by gravity), and the capability of monitoring the physical properties of a specimen from the liquid to the solid state (as in the cure by chemical reaction of a thermosetting resin or on cooling through the glass transition region of a thermoplastic system).

The pendulum is intermittently set into oscillation to generate a series of damped waves as the material properties of the specimen change with temperature and/or time. The free oscillations are initiated by step-displacement of the gear attached to the upper activation rod of the inner pendulum, and the damped oscillations are converted to electrical analog signals by the optical transducer.

The shear modulus, G', is given by

$$G' = KI(2\pi f)^2 \left[1 + \left(\frac{\Delta}{2\pi}\right)\right] \quad (1)$$

where f is the frequency (Hz) of the oscillation, I is the moment of inertia, Δ is the logarithmic decrement [$\Delta = \ln(A_i/A_{i+1})$, A_i is the amplitude of the ith oscillation], and K is a geometric constant. Equation 1 is usually approximated by

$$G' \approx KI(2\pi f)^2 \quad (2)$$

when $\Delta/2\pi < 0.1$. The loss modulus, G", is

$$G'' = \frac{KI\Delta}{\pi}(2\pi f)^2 \quad (3)$$

The loss tangent, tan δ, is a characteristic measure of the ratio of the energy dissipated per cycle to the maximum potential energy stored during a cycle:

$$\frac{G''}{G'} = \tan\delta \approx \frac{\Delta}{\pi} \approx \frac{\alpha}{\pi f} \quad (4)$$

where α is the damping coefficient. During a dynamic mechanical thermal analysis experiment, the moduli can be monitored by observing the changes in the frequency and logarithmic decrement (Δ) of the oscillations. In a torsion pendulum experiment, where the geometric constants are known, the absolute moduli are obtained: [e.g., for a rectangular film,

$$G' = \frac{(2\pi f)^2 IL}{N}\left[1 + \left(\frac{\Delta}{2\pi}\right)^2\right] - \frac{mgb^2}{12N} \quad (5)$$

in which the form factor, N, is

$$N = \frac{a^3 b}{3}\left(1 - 0.63\,\frac{a}{b}\right) \quad (6)$$

where a, b, and L are the thickness, width (a < b/3), and length respectively of the film, g is the gravitational constant, and m is the mass. I can be obtained in a calibration experiment using a wire of known modulus and dimensions]. Although the geometric constants are not known in a TBA experiment, the frequency can be

used to calculate a relative modulus, since $G' \propto f^2$. The TBA plots display the relative rigidity as $1/P^2$ where P is the natural period of the oscillations.

The natural frequency of the oscillations range from 0.01 Hz (for a liquid) to 10 Hz (for a solid), and the logarithmic decrement ranges from 0.001 to 3.0.

The data acquisition system (24) consists of a desktop computer (with printer, plotter, and disc drives), multiplexed switch, and a digital voltmeter, as shown in Figure 7. The computer monitors the temperature and torsion pendulum oscillation signals, controls the initiation of the oscillations, and derives the frequency and logarithmic decrement of the oscillations from the raw data. The reduced data are stored and are available for plotting and/or printing or further massaging.

The computer controls the pendulum in a repetitive sequence, as shown in Figure 8: after monitoring the wave until it has damped out, the computer aligns the pendulum for a linear response by rotating one of the polarizers and then initiates a new oscillation by cocking the pendulum against a spring (via a gear train), again monitoring the wave until the oscillations have decayed, and then releasing it so that the oscillations are centered about the center of the linear region. The wave is digitized and stored until the oscillations have decayed. The frequency and logarithmic decrement are extracted from the digitized wave by, for example, a non-linear least squares fit to the solution of the differential equation of motion:

$$\theta = \theta_o e^{-\alpha t} \cos(2\pi f t + \phi) + Bt + C \qquad (7)$$

where θ is the angular deformation of the pendulum as a function of time t, θ_o is the initial deformation, ϕ is the phase angle, B is the drift coefficient, and C is the offset.

APPLICATIONS

Much of the text of this review can be obtained by of analysis of TBA data. This includes the TTT cure diagram itself (Fig. 1 and Fig. 4), and the T_g versus conversion relationship (Fig. 2). Typical TBA plots for a) the isothermal cure of a liquid epoxy and b) the temperature dependent behavior of a cured epoxy are included in Figures 9 and 10, respectively. Tansition times (e.g., vitrification and macroscopic gelation) and transition temperatures (e.g., T_g) are located by maxima in the mechanical damping (logarithmic decrement) curves. A review of the technique and its application to polymers in general has been published (1,24).

Acknowledgements - Financial support has been provided by the Office of Naval Research.

REFERENCES

1. J. K. Gillham in J. V. Dawkins, ed., Developments in Polymer Characterisation, Vol. 3, Applied Science Publishers, Ltd., London, 1982, Chapt. 5, pp. 159-227.
2. J. K. Gillham, Encyclopedia of Polymer Science and Engineering, Second Edition, 4, 519 (1986).
3. P. J. Flory, Principles of Polymer Chemistry, Cornell University Press, Ithaca, N.Y., 1953.
4. P. G. Babayevsky and J. K. Gillham, J. Appl. Polym. Sci. 17, 2067 (1973).
5. L. C. Chan, J. K. Gillham, A. J. Kinloch, and S. J. Shaw, Adv. Chem. Ser. 208, 235 (1984).
6. Ibid., 261 (1984).
7. S. Wu, Polymer 26, 1855 (1985).
8. J. K. Gillham, P. N. Reitz and M. J. Doyle, Polym. Eng. Sci. 8, 227 (1968).
9. M. B. Roller, Polym. Eng. Sci. 10, 692 (1979).
10. J. B. Enns and J. K. Gillham, Adv. Chem. Ser. 203, 27 (1983).
11. G. Palmese and J. K. Gillham, J. Appl. Polym. Sci. 34, 1925 (1987).
12. X. Peng and J. K. Gillham, J. Appl. Polym. Sci. 30, 4685 (1985).
13. L. C. Chan, H. N. Naé, and J. K. Gillham, Polym. Prepr. Am. Chem. Soc. Div. Org. Coat. Plast. Chem. 48, 566 (1983); J. Appl. Polym. Sci. 29, 3307 (1984).
14. J. D. Ferry, Viscoelastic Properties of Polymers, 3rd ed., John Wiley & Sons, Inc., New York, 1980.
15. H. E. Adabbo and R. J. J. Williams, J. Appl. Polym. Sci. 27, 1327 (1982).
16. J. B. Enns and J. K. Gillham, J. Appl. Polym. Sci. 28, 2567 (1983).
17. M. T. Aronhime and J. K. Gillham, J. Coat. Technol. 56(718), 35 (1984).
18. J. K. Gillham, J. A. Benci and A. Noshay, J. Appl. Polym. Sci. 18, 951 (1974).
19. M. T. Aronhime, X. Peng, J. K. Gillham and R. D. Small, J. Appl. Polym. Sci., 32, 3589 (1986).
20. K. P. Pang and J. K. Gillham, J. Appl. Polym. Sci. In Press (1988).
21. A. F. Lewis, M. J. Doyle and J. K. Gillham, Polym. Eng. Sci. 10, 683 (1979).
22. M. T. Aronhime and J. K. Gillham, J. Appl. Polym. Sci. 29, 2017 (1984).
23. S. Gan, J. K. Gillhan and R. B. Prime, J. Appl. Polym. Sci. In press (1988).
24. J. B. Enns and J. K. Gillham, in T. Provder, ed., Computer

Applications in Applied Polymer Science, Am. Chem. Soc., Symposium Series, No. 197, 329 (1982).

FIGURE CAPTIONS

Fig. 1 Time-temperature-transformation (TTT) isothermal cure diagram for a thermosetting system, showing three critical temperatures, ie, $T_{g\infty}$, $_{gel}T_g$, T_{go}, and the distinct states of matter, ie, liquid, sol/gel rubber, gel rubber (elastomer), gelled glass, ungelled (or sol) glass, and char. The full-cure line, ie, $T_g = T_{g\infty}$, divides the gelled glass region into two parts: sol/gel glass and fully cured gel glass. Phase separation occurs prior to gelation. Successive isoviscous contours shown in the liquid region differ by a factor of ten. The vitrification process below $_{gel}T_g$ has been constructed to be an isoviscous one. The transition region approximates the half width of the glass transition.

Fig. 2 T_g vs conversion at vitrification for reactants differing in functionality (101 > 011). The conversions at molecular gelation are also included. The diagram can be used to demonstrate the effect of increasing functionality of the reactants on molecular gelation, vitrification, and the temperatures $_{gel}T_g$, T_{go}, and $T_{g\infty}$.

Fig. 3 RT density of slow-cooled specimens vs. (T_g - RT) for different isothermal cure temperatures (20): (△) 66.7°C; (▲) 80°C; (□) 100°C; (■) 120°C; (◇) 140°C; (◘) 165°C; (◆) 180°C, and (⊡) 200°C. Arrows indicate vitrification where $T_g = T_{cure}$. Temperature $_{gel}T_g$ (dashed line) is used as a demarcation between ungelled and gelled specimens.

Fig. 4 Summary Time-Temperature-Transformation (TTT) Diagram for a Solvent-Based Reactive Coating System. (Glass transition temperatures ≥ 135°C are bounded as marked.)

Fig. 5 TBA Torsion Pendulum.

Fig. 6 Pendulum Assembly.

Fig. 7 System Diagram.

Fig. 8 Theory of Operation. An analog electrical signal is obtained from a light beam passing through a pair of polarizers, one of which oscillates with the specimen. The pendulum is aligned for linear response and oscillations are initiated by the computer which also processes the damped waves to provide the dynamic mechanical spectrum.
Automated torsion pendulum: control sequence. Key: I, previous wave decays, drift detected and correction begins; II,

reference level of polarizer pair reached; III, wave initiating sequence begins. IV, decay of transients; V, free oscillations begin; VI, data collected; and VII, control sequence repeated.

Fig. 9 Representative TBA Isothermal (100 to 200°C) Cure Spectra of a Rubber-Modified Epoxy System (13). Relative Rigidity (Left) and Logarithmic Decrement (Right) versus Log_{10} Time.

Fig. 10 Sequential TBA Temperature Scans after Isothermal Cure (120°C/36 hr) of a Rubber-Modified Epoxy System (13). Temperature scan: 120 to -170 to 240 to -170°C at 1.5°C/min in dry helium atmosphere. Transition temperatures (°C) and frequencies (Hz) are marked.

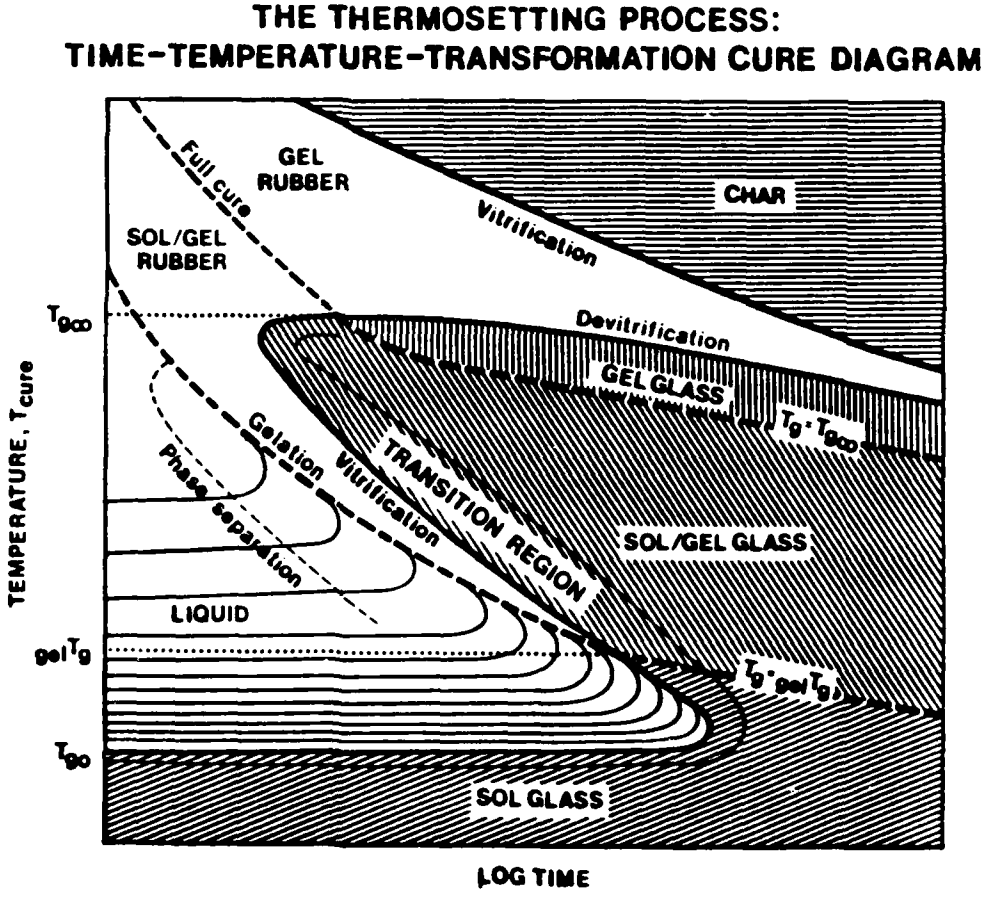

Fig. 1

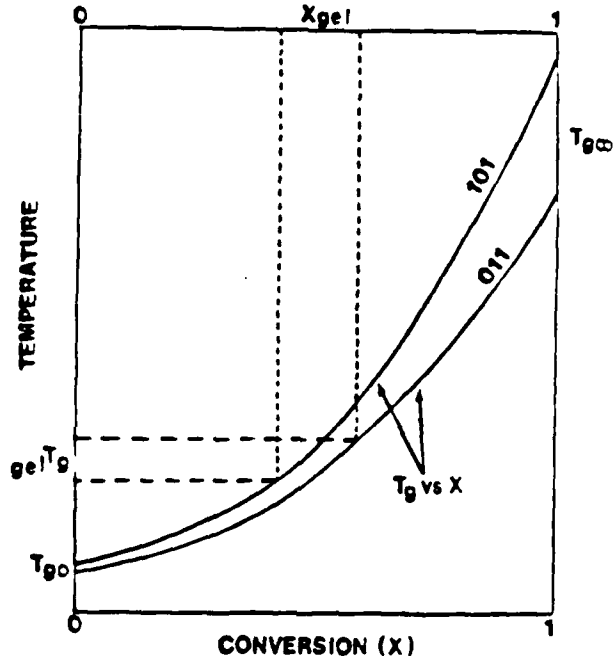
0
X_{gel}
1
$T_{g\infty}$
101
011
TEMPERATURE
$_{gel}T_g$
T_g vs X
T_{go}
0
1
CONVERSION (X)

Fig. 2

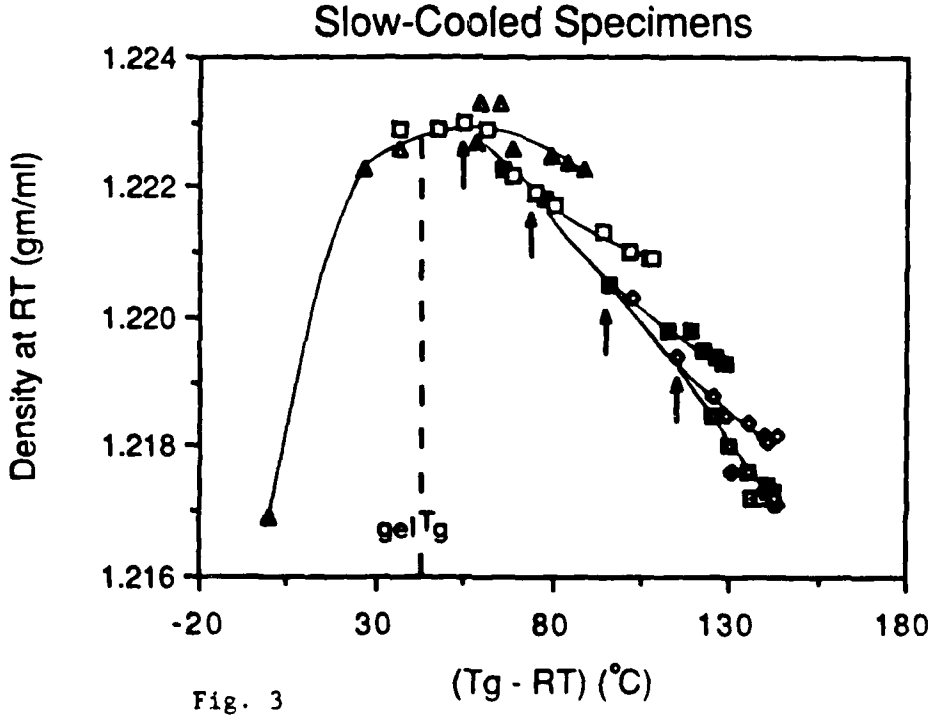
Slow-Cooled Specimens
1.224
1.222
1.220
1.218
1.216
Density at RT (gm/ml)
$_{gel}T_g$
-20
30
80
130
180
(Tg - RT) (°C)

Fig. 3

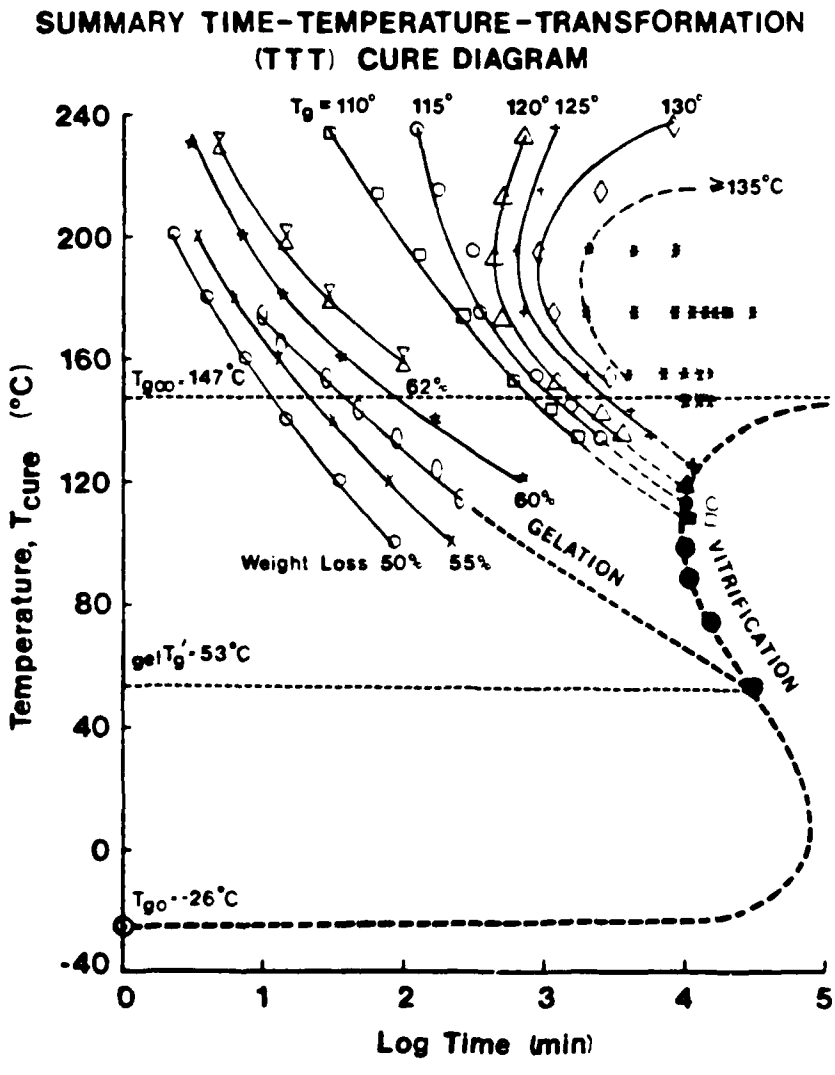
SUMMARY TIME-TEMPERATURE-TRANSFORMATION
(TTT) CURE DIAGRAM
T_g = 110°
115°
120°
125°
130°
≥135°C
240
200
160
120
80
40
0
-40
$T_{g\infty}$ - 147°C
$gel T_g'$ - 53°C
T_{go} - -26°C
62%
60%
Weight Loss 50%
55%
GELATION
VITRIFICATION
Temperature, T_{cure} (°C)
0
1
2
3
4
5
Log Time (min)

Fig. 4

Fig. 5

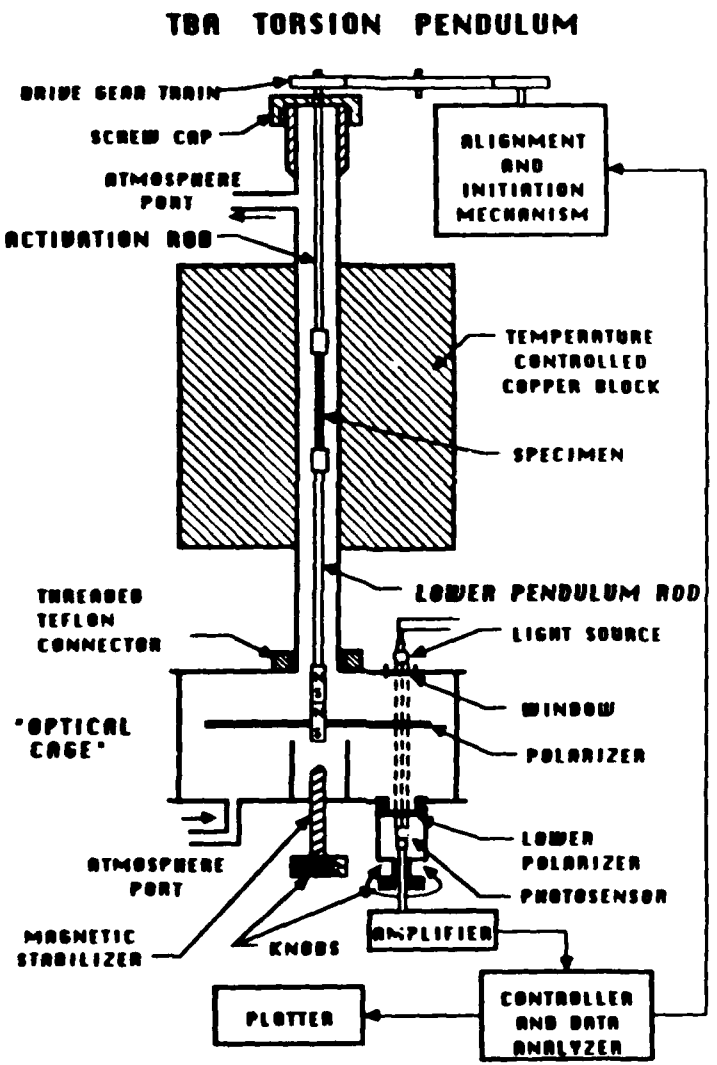
TBA TORSION PENDULUM
DRIVE GEAR TRAIN
SCREW CAP
ATMOSPHERE PORT
ACTIVATION ROD
ALIGNMENT AND INITIATION MECHANISM
TEMPERATURE CONTROLLED COPPER BLOCK
SPECIMEN
LOWER PENDULUM ROD
THREADED TEFLON CONNECTOR
LIGHT SOURCE
WINDOW
"OPTICAL CAGE"
POLARIZER
LOWER POLARIZER
ATMOSPHERE PORT
PHOTOSENSOR
MAGNETIC STABILIZER
KNOBS
AMPLIFIER
PLOTTER
CONTROLLER AND DATA ANALYZER

Fig. 6

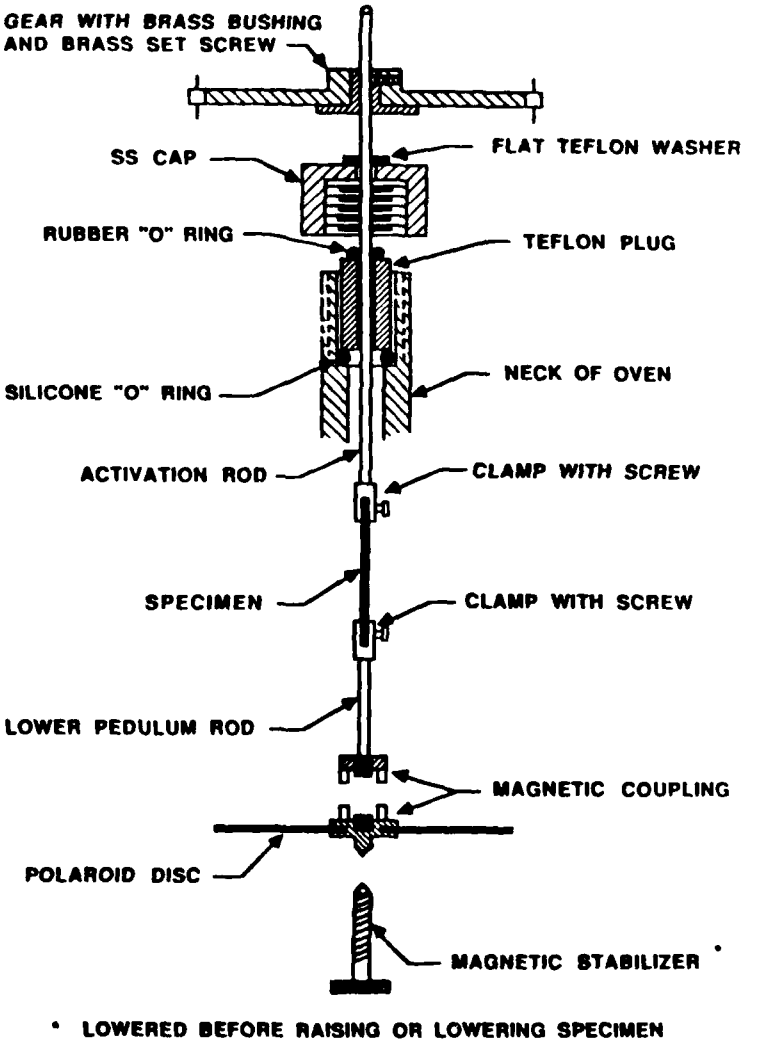
PENDULUM ASSEMBLY
GEAR WITH BRASS BUSHING AND BRASS SET SCREW
SS CAP
FLAT TEFLON WASHER
RUBBER "O" RING
TEFLON PLUG
SILICONE "O" RING
NECK OF OVEN
ACTIVATION ROD
CLAMP WITH SCREW
SPECIMEN
CLAMP WITH SCREW
LOWER PEDULUM ROD
MAGNETIC COUPLING
POLAROID DISC
MAGNETIC STABILIZER *
* LOWERED BEFORE RAISING OR LOWERING SPECIMEN

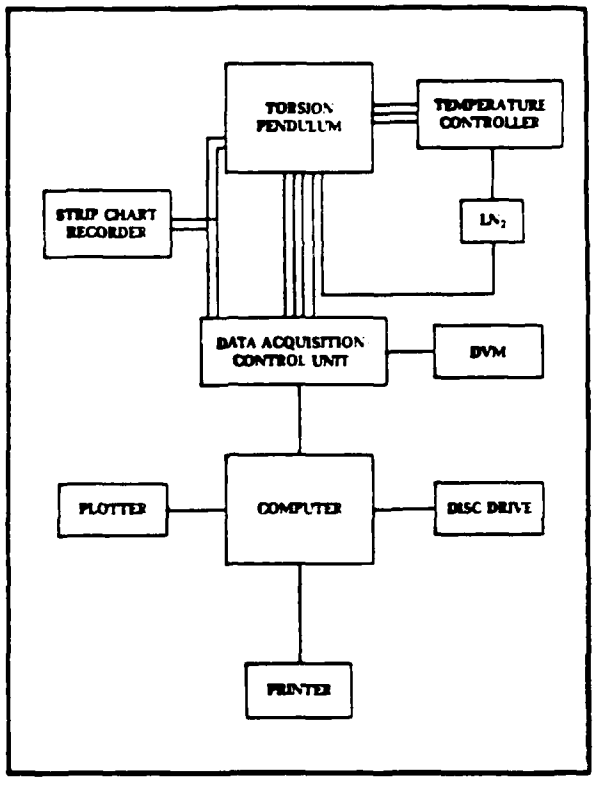
TORSION PENDULUM
TEMPERATURE CONTROLLER
STRIP CHART RECORDER
LN_2
DATA ACQUISITION CONTROL UNIT
DVM
PLOTTER
COMPUTER
DISC DRIVE
PRINTER

Fig. 7

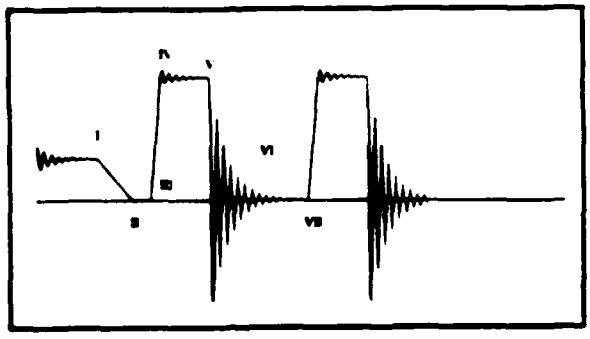

Fig. 8

Fig. 9

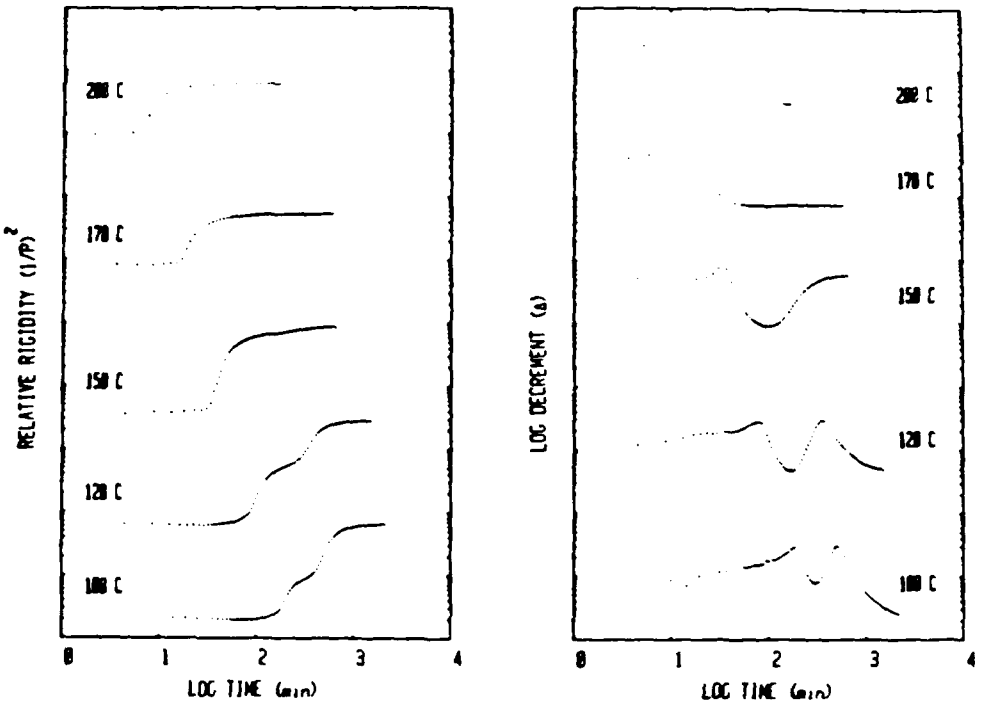
RELATIVE RIGIDITY (1/P)²
LOG DECREMENT (Δ)
LOG TIME (min)
LOG TIME (min)
200 C
170 C
150 C
120 C
100 C
0
1
2
3
4

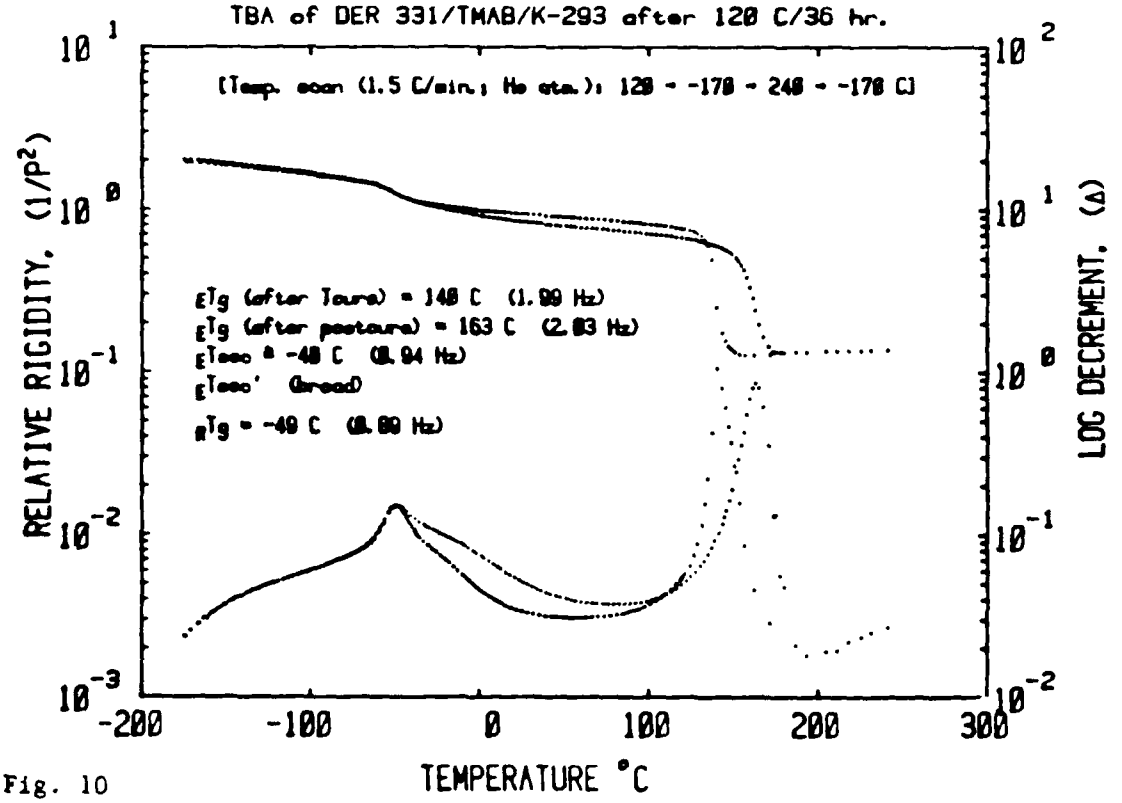
TBA of DER 331/TMAB/K-293 after 120 C/36 hr.
[Temp. scan (1.5 C/min.; He atm.): 120 → -170 → 240 → -170 C]
RELATIVE RIGIDITY, (1/P²)
LOG DECREMENT, (Δ)
TEMPERATURE °C
gTg (after 1cure) = 148 C (1.99 Hz)
gTg (after postcure) = 163 C (2.83 Hz)
gTcc' = -48 C (0.94 Hz)
gTcc' (broad)
gTg = -49 C (0.89 Hz)
10 1
10 0
10 -1
10 -2
10 -3
10 2
10 1
10 0
10 -1
10 -2
-200
-100
0
100
200
300

Fig. 10

DL/1113/87/2

TECHNICAL REPORT DISTRIBUTION LIST, GEN

	No. Copies
Office of Naval Research Attn: Code 1113 800 N. Quincy Street Arlington, Virginia 22217-5000	2
Dr. Bernard Douda Naval Weapons Support Center Code 50C Crane, Indiana 47522-5050	1
Naval Civil Engineering Laboratory Attn: Dr. R. W. Drisko, Code L52 Port Hueneme, California 93401	1
Defense Technical Information Center Building 5, Cameron Station Alexandria, Virginia 22314	12 high quality
DTNSRDC Attn: Dr. H. Singerman Applied Chemistry Division Annapolis, Maryland 21401	1
Dr. William Tolles Superintendent Chemistry Division, Code 6100 Naval Research Laboratory Washington, D.C. 20375-5000	1
Dr. David Young Code 334 NORDA NSTL, Mississippi 39529	1
Naval Weapons Center Attn: Dr. Ron Atkins Chemistry Division China Lake, California 93555	1
Scientific Advisor Commandant of the Marine Corps Code RD-1 Washington, D.C. 20380	1
U.S. Army Research Office Attn: CRD-AA-IP P.O. Box 12211 Research Triangle Park, NC 27709	1
Mr. John Boyle Materials Branch Naval Ship Engineering Center Philadelphia, Pennsylvania 19112	1
Naval Ocean Systems Center Attn: Dr. S. Yamamoto Marine Sciences Division San Diego, California 91232	1

END

DATE

FILMED

5-88

DTIC